

Persistent quantum walks: dynamic phases and diverging timescales

Suchetana Mukhopadhyay¹ and Parongama Sen¹

¹*Department of Physics, University of Calcutta, 92 Acharya Prafulla Chandra Road, Kolkata 700009, India.*

A discrete time quantum walk is considered in which the step lengths are chosen to be either 1 or 2 with the additional feature that the walker is persistent with a probability p . This implies that with probability p , the walker repeats the step length taken in the previous step and is otherwise antipersistent. We estimate the probability $P(x, t)$ that the walker is at x at time t and the first two moments. Asymptotically, $\langle x^2 \rangle = t^\nu$ for all p . For the extreme limits $p = 0$ and 1 , the walk is known to show ballistic behaviour, i.e., $\nu = 2$. As p is varied from zero to 1 , the system is found in four different phases characterised by the value of ν : $\nu = 2$ at $p = 0$, $1 \leq \nu \leq 3/2$ for $0 < p < p_c$, $\nu = 3/2$ for $p_c < p < 1$ and $\nu = 2$ again at $p = 1$. p_c is found to be very close to $1/3$ numerically. Close to $p = 0, 1$, the scaling behaviour shows a crossover in time. Associated with this crossover, two diverging timescales varying as $1/p$ and $1/(1 - p)$ close to $p = 0$ and $p = 1$ respectively are detected. Using a different scheme in which the antipersistence behaviour is suppressed, one gets $\nu = 3/2$ for the entire region $0 < p < 1$. Further, a measure of the entropy of entanglement is studied for both the schemes.

I. INTRODUCTION

Discrete time quantum walks (DTQW's), first introduced by Aharonov *et al.* [1], are random walks where a coin degree of freedom is introduced which determines the translation of the walker. Quantum interference in such walks leads to the position x of the walker scaling as $\langle x^2 \rangle \propto t^2$ with time t , indicating a quadratically faster spread than the classical random walk.

The introduction of randomness or disorder in quantum walks has been demonstrated to modify its scaling behavior significantly. Disorder can be incorporated in various ways, and several studies in recent years have focused on the modifications they impart and how they may turn out to be useful [2]. Disorder introduced through interaction with the external environment or the presence of broken links in position space tends to slow down the quantum walk and leads to localization [3, 4]. Such localization effects were first studied by Anderson [5] in the context of electron localization in a disordered lattice. Anderson localization type behavior has been observed experimentally by introducing static (positional) disorder in a quantum walk on a homogeneous lattice [6]. Static disorder can be contrasted with dynamic disorder or decoherence [4] that transforms the quantum walk to the classical equivalent (diffusive scaling; $\langle x^2 \rangle - \langle x \rangle^2 \propto t$).

Dynamic disorder is usually introduced through the operations controlling the evolution of the quantum walk, such as by using decoherent coins [7, 8]. It is also possible to incorporate dynamic disorder by relaxing the standard assumption of a constant displacement at each time step and allowing longer steps to be chosen randomly, as in [9, 10] where the scaling $\langle x^2 \rangle \propto t^{3/2}$ was found.

In the present work we introduce the concept of persistence in the quantum walk. In a classical random walk, persistence implies that the walker continues in the direction taken in the previous step, making it non-Markovian. In the quantum walk, in order to introduce the idea of persistence, we allow the walker to take different step

lengths at each step and remember the step length chosen in the preceding step with a certain probability. This provides a simple way to study the effect of short term memory in the long-ranged walk. The probability distribution of the position of the walker and its first and second moments are evaluated and the results compared with the classical walk and the quantum walk without disorder. In addition, we evaluate the entropy of entanglement.

Previously, a few studies have been made where memory has been incorporated in different ways in a quantum walk [11–15]. Both short term and long term memory have been considered but in a very different manner. In particular, in the case of the so-called ‘elephant quantum walk’ [14] where the walker has infinite memory as well as time dependent step lengths, the variance was found to scale as t^3 . To the best of our knowledge, the persistence in quantum walks, the way it has been incorporated in the present work, has not been considered before.

In the next section we introduce the quantum walk and the exact way the concept of persistence has been used. In Section III, the results have been presented. Section IV includes a summary of the results and a detailed discussion on the implications and the insight developed through the study.

II. THE PERSISTENT QUANTUM WALK

In the simple DTQW in one dimension, the walker can occupy discrete, equispaced sites x on the real line and takes a step at unit time intervals. In addition to the position, the walker is assigned a second degree of freedom, by means of a coin state (either left ($|L\rangle$) or right ($|R\rangle$)). The state of the walker is described by the following two-component vector expressing probability amplitudes for the coin states:

$$|\psi(x, t)\rangle = \langle x | \psi(t) \rangle = \begin{bmatrix} a(x, t) \\ b(x, t) \end{bmatrix}. \quad (1)$$

The occupation probability of the site x at time step t is given by $P(x, t) = |\langle x | \psi(t) \rangle|^2 = |a(x, t)|^2 + |b(x, t)|^2$ with the total probability is equal to 1 at each time step. A step in the quantum walk consists of a rotation in the coin space followed by a translation. A standard choice for this rotation operator is the Hadamard coin H , given by

$$H = \frac{1}{\sqrt{2}} \begin{bmatrix} 1 & 1 \\ 1 & -1 \end{bmatrix}. \quad (2)$$

Instead of defining the step length to be a constant l , we allow it to be chosen from a binary distribution; $l(t) = \{1, 2\}$ at any given time t . The conditional translation operator at a time t is then written as

$$T(t) = |R\rangle \langle R| \otimes \sum_x |x + l(t)\rangle \langle x + l(t)| + |L\rangle \langle L| \otimes \sum_x |x - l(t)\rangle \langle x - l(t)| \quad (3)$$

Allowing for a non-unique step length in this way enables one to study the phenomenon of persistence by considering the tendency to adopt the step length used in the previous time step. This choice is made in two ways, outlined under two different schemes, I and II. In each scheme, at $t = 0$, the step length $l(0) = 1$ or $l(0) = 2$ is chosen with equal probability. In Scheme I, at any later time $t \neq 0$, the walker either chooses the same step length as in the previous time step (persistent) and otherwise necessarily chooses the other step length (anti-persistent). In Scheme II, the walker is persistent with a probability p , but this time with probability $(1 - p)$, either of the step lengths $l = 1$ and $l = 2$ are chosen, with probability q and $(1 - q)$ respectively.

For both schemes the walker is initialised with $a(x, 0) = b(x, 0) = \frac{1}{\sqrt{2}}\delta_{x,0}$ which gives an asymmetric probability distribution profile in the absence of disorder. The walk is evolved for 20000 time steps for all parameter values. We investigate how the occupation probability, moments, and entanglement depend on the parameter(s) used in the two schemes. All results are averaged over 4000 configurations.

III. RESULTS

A. Scheme I

In this subsection we present the results for the first scheme considered. The walker here chooses the step length taken in the previous step with probability p and with probability $(1 - p)$ it chooses strictly the other length. The latter case thus corresponds to an antipersistent choice.

1. Probability distribution

When $p = 0$, steps of length $l = 1$ and 2 are taken alternately, with a possible sequence of steps given by $1, 2, 1, 2, 1, \dots$ etc. The walk clearly has periodicity 2, and there is no randomness in the choice of steps. This particular walk has already been studied in [9] and was found to have the same scaling behavior as the ordinary quantum walk. The probability distribution resembles an overlap of distributions obtained for the ordinary walks with $l = 1$ and 2 [9].

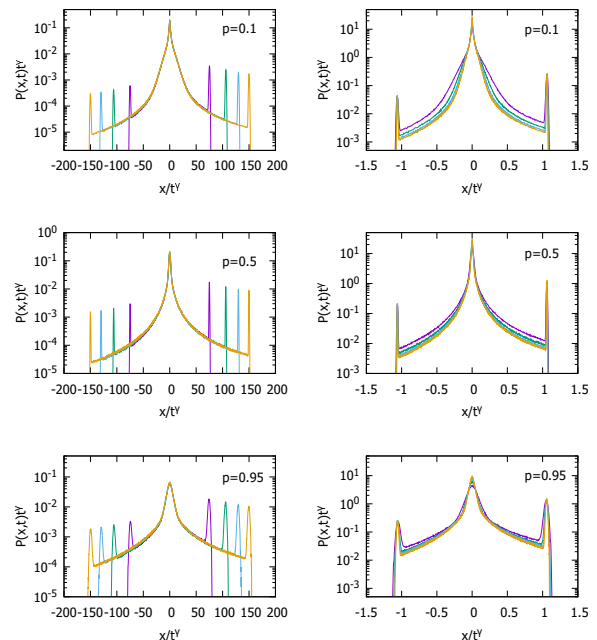


FIG. 1. Scheme I : Data collapse of rescaled $P(x, t)$ using $\gamma = 0.5$ (left column), $\gamma = 1.0$ (right column). $\gamma = 1$ collapse is less sharp.

On the other hand, when $p = 1$, the walk becomes deterministic with a unique step length and thus identical to the usual quantum walk. The result for the point $p = 0.5$ can also be easily guessed. Here essentially the step lengths 1 and 2 are being chosen with equal probability at each step. Hence it belongs to the class of models studied in [9].

As p is increased even slightly from zero, the distribution $P(x, t)$ exhibits a peak centered at the origin in addition to two ballistic peaks. Such a central peak is not present in the ordinary quantum walk, neither in the binary walk without randomness. However, in presence of disorder and decoherence, such peaks indeed appear, when localisation of the quantum walker takes place.

The ballistic peaks are signatures of the quantum nature of the walk, and are in general asymmetric in height, reflecting the asymmetry of the pure quantum walk. As p is increased, the ballistic peaks are seen to increase in height, while the central peak goes down. This can be in-

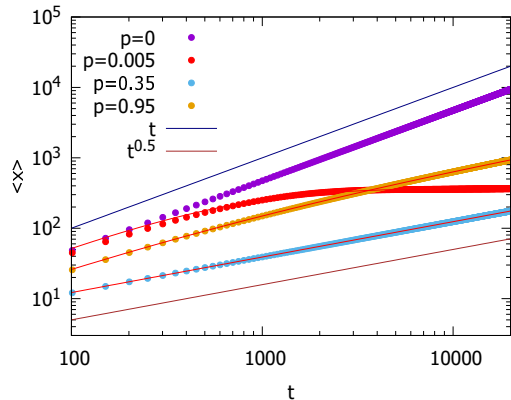


FIG. 2. Scheme I: The first moments for four p values show significant change in behaviour as p is varied.

terpreted as an increase in delocalisation with increasing probability of the walker to be persistent, as the walker approaches the standard case of a constant step length. Even for p very close to one, however, the central peak does not disappear. Exactly at $p = 1$, the familiar distribution of the quantum walk is recovered, as expected.

Plotting $t^\gamma P(x, t)$ against the scaled variable x/t^γ , we observe data collapse for four different time steps, with $\gamma = 0.5$ for the central peak and $\gamma = 1.0$ for the ballistic peaks. We conclude that $P(x, t)$ exhibits two distinct scaling behaviors: the centrally peaked part scales as $x \propto \sqrt{t}$, similar to the classical walk, while the ballistic peaks scale like the ordinary quantum walk, $x \propto t$. These results are true for the entire region $0 < p < 1$ as shown in Fig. 1.

2. Scaling of the moments

We next present the results for the first two moments, $\langle x \rangle$ and $\langle x^2 \rangle$ of the probability distribution.

In the limiting cases of $p = 0$ and $p = 1$, the walk reduces to an ordinary quantum walk such that $\langle x \rangle \propto t$ and $\langle x^2 \rangle \propto t^2$. Interestingly, when p deviates from zero or one by even the smallest amount, we note that the asymptotic variations of the moments are significantly changed. The first moments are plotted in Fig. 2 for a few p values, showing that the asymptotic exponent decreases to very small values for $p = 0^+$ and increases up to a value close to $1/2$ at larger p values.

We plot the second moments in Fig. 3 for a few values of p . Usually it is the variance which is used to characterise the walk. However, we note here that asymptotically, $\langle x^2 \rangle$ is larger than $\langle x \rangle^2$ by at least two orders of magnitude. Hence it suffices to consider how $\langle x^2 \rangle$ behaves instead of the variance $\langle x^2 \rangle - \langle x \rangle^2$. In the following, we study the behaviour of the second moment in detail.

We note two things from Fig. 3; first, for p values close to zero and 1, there is a distinct change in the behaviour of the moments with time; initially it has a fast growth

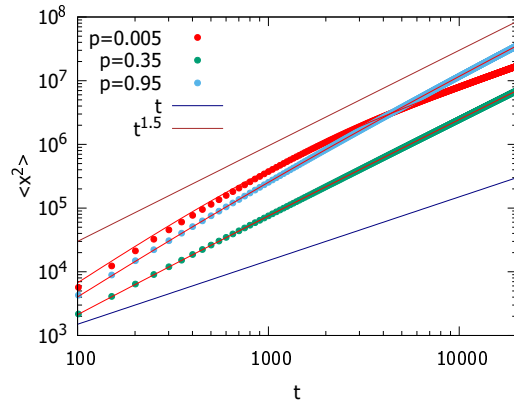


FIG. 3. Scheme I: The second moment for three p values. The continuous lines are best fit curves obtained using Eq. 5 with fitting parameters $\alpha' = 1.379, 0.81, 1.81$ and $\beta' = 0.0011, 0.382, 0.066$ for $p = 0.005, 0.35$ and 0.95 respectively.

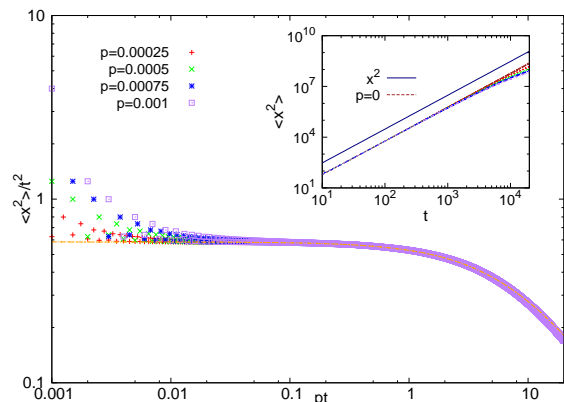


FIG. 4. Scheme I: Data collapse of the second moment of the distribution $P(x, t)$ obtained on plotting $\langle x^2 \rangle / t^2$ against the scaling variable pt . The solid line is a best fit line drawn using Eq. 4. Inset shows the unscaled data $\langle x^2 \rangle$ against time t . The data for $p = 0$ and a curve with quadratic variation are shown for comparison.

but becomes slower later. Secondly, the asymptotic variation is significantly dependent on p ; for a value of p very close to zero, the exponent is close to 1. This is a drastic change from the value 2 when p is exactly zero.

We probe the $p \rightarrow 0^+$ region in more detail as we have the most significant change in the asymptotic exponent value here. Here, $\langle x^2 \rangle$ plotted in the inset of Fig. 4, clearly shows a variation compatible with t^2 for a long time before deviating to a slower variation. The deviation occurs at larger values of time as p approaches zero. Plotting $\langle x^2 \rangle / t^2$ against the scaling variable pt for several values of p very close to zero, we obtain a very good collapse (Fig. 4) from which we claim $\langle x^2 \rangle \propto t^2 f(pt)$. It is clear from Fig. 4 that $f(z)$ is fairly a constant for $z < 1$. For $z \geq 1$, one can fit $f(z)$ to the form

$$f(z) = 1/(\alpha + \beta z^\mu) \quad (4)$$

to a great degree of accuracy with $\alpha \approx 1.7, \beta \approx 0.2$ and $\mu \approx 1$. From this it can be concluded that a crossover occurs at $pt \approx 1$ and there is a diverging time scale varying inversely with p . On the other hand the asymptotic variation is $\langle x^2 \rangle \propto t$. Thus the crossover time marks the transition to the asymptotic behaviour.

As p is made larger, the crossover occurs at smaller times and the exponent is extracted from fitting the second moment directly to the empirical form valid for later times:

$$\langle x^2 \rangle = t^2 / (\alpha' + \beta' t^{2-\nu}), \quad (5)$$

such that asymptotically, $\langle x^2 \rangle \propto t^\nu$. The best fit curves using the above form plotted for the data shown in Fig. 3 show excellent agreement. In Fig. 5, the asymptotic exponents ν is plotted as a function of p . One notes that the exponent continuously varies from 1 to $3/2$ in the region $0 < p < p_c$ where p_c is approximately 0.33.

A similar crossover is noted close to $p = 1$, where also the exponent shows a jump from the value 2 to $\sim 1/2$. Here the scaling variable is $(1-p)t$ such that the associated timescale diverges as $\frac{1}{1-p}$.

We note therefore that the walk shows a superdiffusive behaviour but with a nonuniversal exponent for small p where the antipersistent effect is strong. For larger values of p , the walker behaves as that with random step lengths and persistence is apparently merely the tool that provides the stochasticity. Since it was found in [9] that the slightest randomness alters the exponent to $3/2$, it is not surprising to see that for large $p \neq 1$, one gets the same exponent.

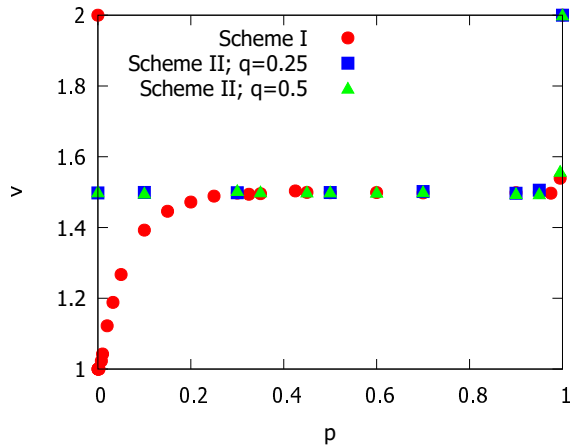


FIG. 5. Variation of the effective scaling exponent ν with p for Scheme I and Scheme II.

3. Entanglement entropy

In any quantum walk, the evolution operator generates entanglement between the position and coin degrees of freedom. This entanglement can be quantified using the

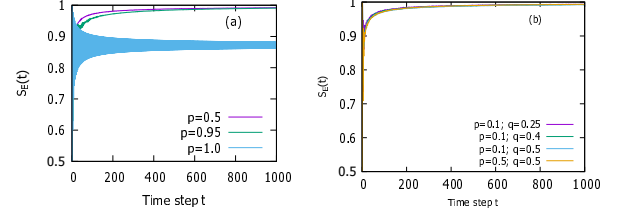


FIG. 6. Entanglement entropy plotted against time for Scheme I (a) and Scheme II (b).

von Neumann entropy $S_E(t)$, also known as the entropy of entanglement. This can be evaluated from the reduced density operator which is represented by the following matrix [16]

$$\rho_c(t) = \begin{bmatrix} A(t) & B(t) \\ B(t) & C(t) \end{bmatrix} \quad (6)$$

where we have $A(t) \equiv \sum_x |a(x,t)|^2$; $B(t) \equiv \sum_x |a(x,t)||b(x,t)|$; $C(t) \equiv \sum_x |b(x,t)|^2$. The entropy of entanglement $S_E(t)$ is then calculated as

$$\begin{aligned} S_E(t) &= -\text{Tr}(\rho_c \log_2 \rho_c) \\ &= -(v_1 \log_2 v_1 + v_2 \log_2 v_2). \end{aligned} \quad (7)$$

where v_1 and v_2 are the real, positive eigenvalues of the matrix $\rho_c(t)$. We numerically evaluate $S_E(t)$ for the quantum walk with the localised initial condition $a(0,0) = \frac{1}{\sqrt{2}}$, $b(0,0) = \frac{1}{\sqrt{2}}$, taking $0 \log_2 0 = 0$. For a constant step length, when $p = 1$, $S_E(t)$ is found to asymptotically converge to $\approx 0.872...$ for our chosen initial condition, as has been previously reported [16–18]. For $p = 0$, we obtain $S_E(t) \approx 0.85...$. As the walk deviates from either of the two extremes, the value of $S_E(t)$ increases drastically, rapidly converging to a large value very close to unity for any p . Although the parameter p does not significantly influence the limiting value (at least not up to three decimal places), the rate of convergence is faster for smaller p values. Fig. 6 shows the behavior of the entanglement for a few values of p .

B. Scheme II

This scheme represents a variation of the first where the walker is either persistent with probability p or, with probability $(1-p)$ can choose step length $l = 1$ or 2 with probability q and $(1-q)$ respectively. Obviously, for $p = 1$ it is always persistent and one recovers an ordinary quantum walk. For $p = 0$, it takes step lengths 1 and 2 randomly unless $q = 0$ or 1 . In fact, if $q = 0$ or 1 , the walk becomes of unique step length eventually, (independent of p); if $q = 1$, that length is 1 and 2 for $q = 0$.

Effectively, the total persistence probability p' of the walker in this scheme is either $p + q(1-p)$ or $p + (1 -$

$q)(1-p)$ at a given time step and it is antipersistent with probability $1-p'$. When $q = 0.5$, the walker is thus persistent with a probability $p' = p/2 + 1/2$ independent of q , and the results should correspond to those obtained for a persistence probability p' in Scheme I. Since $p' > p_c$, one can expect that the results for Scheme II will be identical to Scheme I with the second moment scaling as $t^{3/2}$ asymptotically for all $p \geq 0$. Even when $q \neq 0.5$, the walk is persistent with probability $p/2 + 1/2$ on an average and antipersistent otherwise. Thus one can expect that it will again be equivalent to Scheme I (with persistence probability p'), when ensemble average is taken if the fluctuation is negligible. In the following we discuss the results which confirms the above picture.

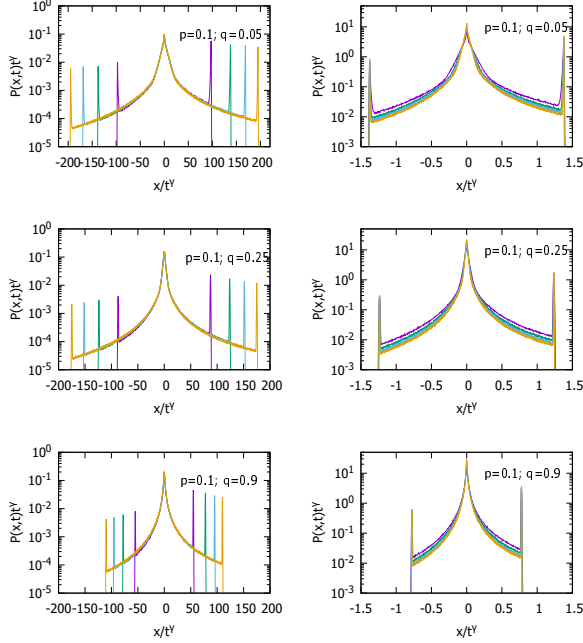


FIG. 7. Scheme II: Data collapse of rescaled $P(x,t)$ using $\gamma = 0.5$ (left column) and $\gamma = 1.0$ (right column). $\gamma = 1$ collapse is less sharp.

Once again we obtain the distribution $P(x,t)$ which shows a peak centered at the origin and two ballistic peaks. As seen for Scheme I, data collapse is observed with $\gamma = 0.5$ for the central peak and $\gamma = 1.0$ for the ballistic peaks (Fig. 7) indicating two distinct scaling behaviors $x \propto \sqrt{t}$ and $x \propto t$ respectively.

Next we show the variation of the second moment in Fig. 8 against time which shows the unique exponent $3/2$ asymptotically for all $0 < p < 1$. Here we have plotted the results for both small and large values of p, q showing no significant difference. The exponent ν as a function of p for $q = 0.5$ and a different value of q plotted in Fig. 5 shows that it is $3/2$ for the entire region $0 < p < 1$, confirming that it is equivalent to Scheme I when the persistent probability for the latter is above p_c .

Lastly, we plot $S_E(t)$ against time t for chosen values of p and q (Fig. 6) which does not show any distinguishing

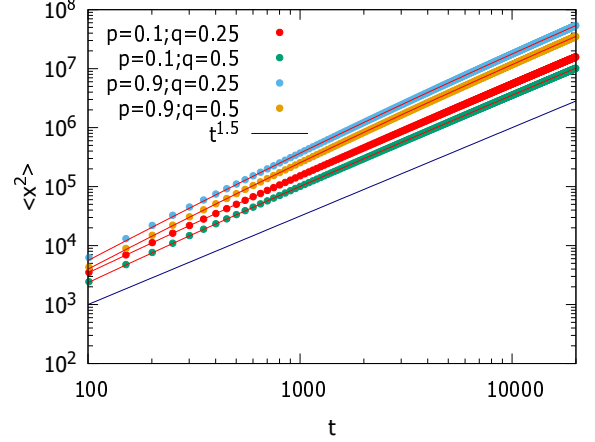


FIG. 8. Scheme II: The second moment for a combination of values of p and q . The continuous lines are best fit curves obtained using Eq. 5.

feature from Scheme I.

IV. SUMMARY AND DISCUSSIONS

In the present work we have reported the results on a non-Markovian quantum walk where the step lengths are binary at each time step. It is non-Markovian in the sense that the walker remembers the step length taken in the previous step and tends to repeat it with probability p . Thus the choice of the step length is entirely determined by the value of p . We numerically evaluate the time evolution of the walk and calculate the distribution $P(x,t)$ and its moments. Scheme I, which is the case when it is strictly antipersistent with probability $(1-p)$, leads to some non-intuitive results when p is small. Precisely, we find how the asymptotic behaviour of the second moment changes as p is varied. One can locate four different phases through which ν changes. The first is the point $p = 0$, where the walk is periodic and correlated over infinite time range and $\nu = 2$. At $p = 0$, there is however, a finite discontinuity in ν as $\nu = 1$ for $p = 0^+$. For $0 < p < p_c$, ν shows a continuous increase with p . Here the walk deviates from its periodic nature and the step lengths are e.g., 1, 2, 1, 2, ..., 1, 2, 2, 1, 2, 1, ..., 1, 1, 2, 1, 2, ... etc., such that it has two “opposite” patterns repeating alternately. However, the long time correlation is weakened. As p increases, the step lengths tend to repeat, however, none of the strings, either e.g., 1, 1, 1...1 or 1, 2, 1, 2, 1, 2 can have a very large length when p is not equal to 1 or zero. As a result, one gets approximately a random sequence of step lengths. In fact at $p = 0.5$ it is purely random. This randomness continues to dominate unless p is exactly equal to 1 so that we get $\nu = 3/2$ for $p_c < p < 1$ and $\nu = 2$ again at $p = 1$.

The result for the region $0 < p < p_c$ is perhaps the

most interesting where we find a p dependent value of $\nu < 3/2$ that indicates that the localisation is stronger compared to a random choice of the step lengths. The antipersistence effect here is able to confine the walk to a narrower region.

Let us further review the situation close to the extreme values of p regarding the step lengths 1 and 2 as up/down states of a Ising spin. The two sequences 1, 2, 1, 2, ... and 2, 1, 2, 1, ... are like antiferromagnetic patterns and are equivalent to simply spin flipped versions of one another in this picture. Hence close to $p = 0$ we have two alternating antiferromagnetic patterns and close to $p = 1$ we will have two alternating ferromagnetic patterns separated by domain boundaries. Interestingly for $p \rightarrow 0$ and $p \rightarrow 1$ the exponents have different values, indicating the antiferromagnetic patterns are responsible for a stronger confinement of the walk. For close to $p = 1$, the confinement comes only from the fact that the repetition of the two ferromagnetic patterns is in no way periodic in nature. However, why the antiferromagnetic and ferromagnetic sequences lead to different scaling behaviour and why p_c is close to $1/3$ remain issues to be resolved. One other result is that in general the first moment shows a scaling $\langle x \rangle \propto t^{\nu-1}$ which is not quite obvious.

The second important result we obtain is the crossover phenomena near $p = 0$ and 1. Simple power law scalings for the moments are not possible here as clearly the behaviour changes in time. Of course, one can continue the numerical evolution for even larger number of time steps

and extract the asymptotic variation. In practice, it is beyond the computational capacity to do so. However, identification of the scaling variable and consequently obtaining a form of the scaling function could help in calculating the asymptotic exponent. We could detect the presence of timescales which diverge at the extreme limits and in the process reveal that the crossover phenomena takes place here with a diverging time scale. This divergence signifies that although the exponent ν changes discontinuously as $p \rightarrow 0$ or $p \rightarrow 1$, the change can be observed only after long time scales. Away from the extreme limits, the crossover effect becomes less conspicuous.

The results for the persistent quantum walker shows that it is clearly different from the case of random choice of step lengths as long as antipersistence is strong, resulting in a nonuniversal value of the exponent. This is all the more evident from the results of Scheme II in which the effective persistence probability corresponds to that in Scheme I with $p > 1/2$ and hence corresponds to the random case with $\nu = 3/2$. Although the scaling exponent ν is p dependent for $p < p_c$, the $P(x, t)$ data show collapse with the same type of rescaling as in the random case. Also, the results for the entanglement entropy are qualitatively similar to that of the latter case.

Acknowledgement:

SM is grateful for the opportunity to work in the Department of Physics, University of Calcutta. PS is grateful to SERB scheme number: EMR/2016/005429.

-
- [1] Y. Aharonov, L. Davidovich, and N. Zagury, Phys. Rev. A **48**, 1687 (1993).
 - [2] V. Kendon, Mathematical Structures in Computer Science **17**, 1169 (2007).
 - [3] J. P. Keating, N. Linden, J. C. F. Matthews, and A. Winter, Phys. Rev. A **76** (2006).
 - [4] Y. Yin, D. E. Katsanos, and S. N. Evangelou, Phys. Rev. A **77**, 022302 (2008).
 - [5] P. W. Anderson, Phys. Rev. **109**, 1492 (1958).
 - [6] A. Schreiber, K. N. Cassemiro, V. Potoček, A. Gábris, I. Jex, and C. Silberhorn, Phys. Rev. Lett. **106**, 180403 (2011).
 - [7] T. A. Brun, H. A. Carteret, and A. Ambainis, Phys. Rev. Lett. **91**, 130602 (2003).
 - [8] T. A. Brun, H. A. Carteret, and A. Ambainis, Phys. Rev. A **67**, 032304 (2003).
 - [9] P. Sen, Physica A **514**, 266 (2019).
 - [10] P. Sen, (2019), arXiv:1902.09129 [quant-ph].
 - [11] M. McGettrick, Quantum Information and Computation **10**, 0509 (2010).
 - [12] P. P. Rohde, G. K. Brennen, and A. Gilchrist, Phys. Rev. A **87**, 052302 (2013).
 - [13] D. Li, M. Mc Gettrick, F. Gao, J. Xu, and Q.-Y. Wen, Phys. Rev. A **93**, 042323 (2016).
 - [14] G. Di Molfetta, D. O. Soares-Pinto, and S. M. D. Queirós, Phys. Rev. A **97**, 062112 (2018).
 - [15] M. A. Pires, G. D. Molfetta, and S. M. D. Queirs, (2019), arXiv:1907.12696 [quant-ph].
 - [16] G. Abal, R. Siri, A. Romanelli, and R. Donangelo, Phys. Rev. A **73**, 042302 (2006).
 - [17] I. Carneiro, M. Loo, X. Xu, M. Girerd, V. Kendon, and P. L. Knight, New Journal of Physics **7**, 156 (2005).
 - [18] G. Abal, R. Siri, A. Romanelli, and R. Donangelo, Phys. Rev. A **73**, 069905 (2006).